INORGANIC GELS WITH NANOMETER-SIZED PARTICLES

B. J. TARASEVICH, J. LIU, M. SARIKAYA, AND I. A. AKSAY

Department of Materials Science and Engineering, and
Advanced Materials Technology Program, Washington Technology Center
University of Washington, Seattle, WA 98195

ABSTRACT

Fundamental issues involving interactions and packing of nanometer-sized particles are being investigated as an extension of previous experimental studies on larger submicron particles and in relationship to general theoretical work on colloidal systems. Relationships between particle interaction energies and packing indicate (1) dense gels can be formed in stable systems by minimization of the hydrodynamic radius and (2) dense clusters can be formed in flocculated systems by the use of weakly attractive particles where particle restructuring occurs. Novel techniques for the formation of nanostructures within polymeric matrices are also introduced to address gel cracking problems.

INTRODUCTION

There has been a growing interest in the colloidal processing of ceramics with submicron-sized particles for the microdesigning of a wide range of single-phase and composite materials [1-3]. Studies have shown that when particle interactions are controlled, highly dense (> 70 v/o) and uniform packing of particles is possible [4]. However, when the particle size is reduced below 0.1 µm, there appears to be an intrinsic difficulty in the preparation of highly concentrated suspensions and high density gels [5,6]. It has been customary to expect that the use of nanometer-sized particles always results in the formation of low density gels that display large drying and sintering shrinkage and subsequent cracking and incomplete sintering [5,6].

If nanometer-sized particles can be packed densely to reduce shrinkage and cracking problems, their use has many advantages over the use of larger submicron-sized particles. One advantage is that inorganic components can be mixed on a nanometer scale to tailor structures with enhanced spatial resolution for increasingly complex electronic, structural, and optical systems. Another advantage is that fully dense materials can be processed at much lower temperatures than can be achieved by conventional processing methods.

Mat. Res. Soc. Symp. Proc. Vol. 121. ©1988 Materials Research Society

The purpose of this paper is to illustrate that many of the processing difficulties associated with nanometer-sized particles result from a lack of fundamental understanding of the factors affecting gel and cluster densities, and that dense structures can be formed by controlling particle interactions. We emphasize two approaches to the formation of dense gels and clusters from nanometer-sized particles; (1) the minimization of the hydrodynamic radius and (2) enhanced restructuring of clustered networks. First, we illustrate the role of the hydrodynamic radius in studies of electrostatically stabilized colloidal silica. Next, we illustrate the importance of cluster restructuring in studies on gold particles aggregated by coating particles with surfactants. In the last section we introduce a novel technique for processing nanostructures by the precipitation of silicate structures within polymeric matrices to provide an alternate solution to the cracking problems associated with the excessive shrinkage of low density gels.

GEL SYSTEMS WITH ELECTROSTATICALLY STABILIZED COLLOIDS

Most of the studies on colloidal silica particle systems have involved the use of particles under very restricted interaction energy conditions, either highly attractive under high electrolyte concentrations [7] or highly repulsive at high pH [8]. We have done studies on packing of silica gels at low electrolyte concentration over a range of interaction energies. Figure 1 shows packing densities as a function of pH for ~160 Å amorphous Ludox silica particles with 10^{-3} M $NaNO_3$ electrolyte. Particles were consolidated under a centrifugal force field and packing densities were measured in the wet state before drying. The inset shows mobility values as a function of pH determined by electrophoresis. Zeta potential values were calculated using the Hückel equation [9] for low κa where the Debye-Hückel length, $1/\kappa$, is large relative to the particle radius, a.

These results are surprising because the lowest packing densities occur at the highest pH where the particles have the highest zeta potentials. This is opposite to the trends seen in larger submicron oxide particles [2]. Viscosity experiments indicated that the suspensions at high pH have the highest viscosities, corresponding to the low packing densities, but the viscosity is greatly reduced by the addition of higher concentrations of electrolyte. A micrograph of pH 9 particles dried on carbon grids is shown in Figure 2 and indicates that these particles form densely packed structures after drying but are still separated by large interparticle distances of about 20 to 30 Å.

This type of densely packed structure with large interparticle separation distances has been confirmed by neutron scattering experiments [10] and is similar to the liquid-like structures seen in highly repulsive polystyrene systems [11]. The low packing density at high potential, therefore, is due to the presence of a large electrostatic double layer as a result of the high charge and long range electrostatic repulsion energies. The double

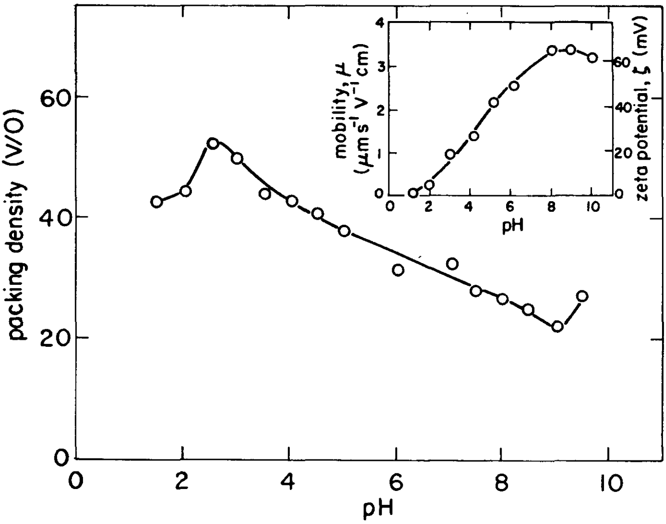

Figure 1. Gel packing densities and zeta potentials of nanometer size silica particles as a function of pH (10^{-3}M $NaNO_3$).

layer results in a large effective hydrodynamic radius, much larger than the particle diameter. Although the particle plus double layer packs densely as shown in Figure 2, the overall packing density is reduced due to the volume occupied by the double layer. The presence of double layer interactions at high pH also explains the high viscosities due to electroviscous effects.

As the pH is lowered from pH 9, the gel packing density increases and the suspension viscosity decreases. This corresponds to the compression of the hydrodynamic radius with decreasing potential. Above pH 9, the presence of excess counterions due to base addition also compresses the hydrodynamic radius, again resulting in an increase in packing density.

Relationships between particle surface potential and packing density are plotted in Figure 3 for data at high charge (above pH 6) as zeta potential, ζ, versus particle number density. This plot can be thought of as a phase diagram of density transitions from suspension to consolidated gel states as a function of particle-particle interactions. This phase diagram is similar to experimental phase diagrams obtained for highly charged polystyrene latices of transitions from disordered to ordered, colloidal crystalline

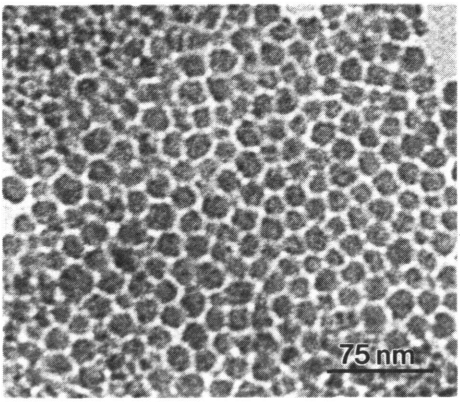

Figure 2. TEM micrograph of nanometer-size silica particles at high zeta potential (pH 9) clustered on carbon grids.

states [12, 13]. Our phase diagram also agrees with the trends of the theoretical phase diagram calculated for highly repulsive systems by a free energy minimization method [14] as shown in Figure 4.

These diagrams indicate that the transitions from disordered to ordered colloidal states in Figure 4 or suspension to gel states in Figure 3 occur at increasing packing density with decreasing charge. In addition to using packing density data of consolidated particles, we found transitions from suspension to gel states by measuring the storage modulus, G′, and loss modulus, G″, of samples by oscillatory shear rheology [15]. Transitions from viscous suspension states ($G'' < G'$) to elastic gel states ($G' > G''$) occur as a function of particle concentration. This transition occurs at increasing particle concentration with decreasing charge in agreement with the packing density results. This also indicates that in repulsive nanoparticle systems, the gel transition, as evidenced by the onset of elastic rheological behavior, occurs as a function of particle concentration.

Although the hydrodynamic effect due to long range repulsive interactions has been seen in larger submicron silica particles at high charge, the effect is much more extreme in reducing packing densities in nanometer size particles. This occurs because the size of the double layer is significant relative to the particle size. Our results, therefore, indicate that highly charged, highly stable systems are not desirable for nanometer particle processing, in contrast to the conventional processing schemes used for larger submicron particle systems.

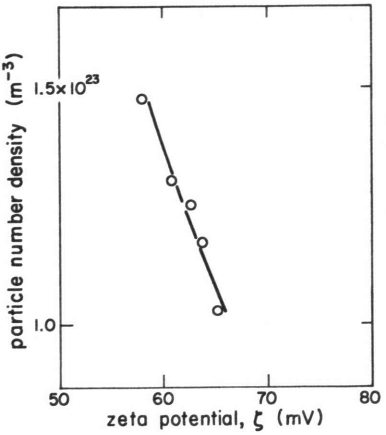

Figure 3. Silica gel particle number densities versus ζ.

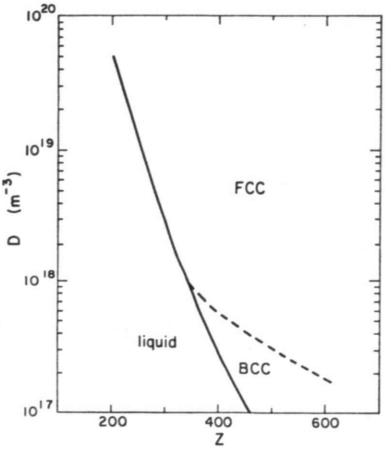

Figure 4. Theoretical phase diagram of transitions from liquid to crystalline states for highly repulsive colloidal systems (from [14]).

The packing density results in Figure 1 indicate that the highest packing occurs at a pH of 2.5. Here we are able to form colloidal gels with packing densities as high as 52 v/o, much higher than those reported in the literature [6]. This result is surprising because particles at low pH have the lowest charge and are predicted by the DLVO theory to have primarily attractive interactions [16]. We found these particles to be stable over long time periods by light scattering, in contrast to submicron silica particles which flocculate at pH 2.5. The stability of nanosize silica particles is well known [17] and has been associated with the adsorption of water molecules onto surface silanol sites, which predominate at low charge. The hydrated layer has been thought to induce short range steric repulsion. This results in stability of nanometer size particles because the van der Waals attraction can be screened by very small steric layers, as small as 5-10 Å.

The mechanism by which bound water layers result in short range repulsion will not be addressed here although this issue is widely discussed and debated and details can be found in the literature [18, 19]. Regardless of the mechanism, the stability of nanosize particles at low charge, as opposed to submicron particles, results in extremely high gel packing densities. It is likely that the hydrophilic behavior of silica particles at low charge is also very important to the complicated aggregation behavior observed under high electrolyte concentrations [17, 20].

Our results for silica packing densities at low pH are similar to the trends for refractive indices of dried thin films reported for another silica system [21]. At high pH, however, high refractive indices occur, corresponding to high gel densities. Although we report very low wet gel densities at high pH, we have evidence for high dried gel densities indicating compression of the hydrodynamic radius during drying.

Our results for Ludox silica at low salt concentration indicate that particle interactions are primarily repulsive. These interactions are dominated by long range electrostatic repulsion or hydrophobic behavior at high charge and short range repulsion or hydrophilic behavior at low charge. Although particles plus double layer order densely at high charge, the hydrodynamic radius greatly lowers wet gel packing densities. Although high densities are achieved after drying, this only occurs after large shrinkages. High wet gel packing densities can be achieved when the hydrodynamic radius is reduced and the particles are stable due to short range repulsion. The presence of long range double layer effects and short range repulsion, as well as attractive interactions have also been observed in our studies on boehmite gels [15].

Since our work demonstrates that the effect of the hydrodynamic radius on packing densities is significant in nanosize particles even at medium potentials (<60 mV), nanoparticle processing should be directed toward reduction of particle surface charge. This can be accomplished by reducing the pH as discussed above for silica resulting in stable systems, or by modifying charge by the adsorption of surfactants as discussed below for gold particles resulting in weakly attractive systems.

AGGREGATION OF SURFACTANT MODIFIED PARTICLES

In this section, we present results on the use of surfactants to form weakly attractive particles that allow the formation of densely packed clusters [22]. The use of clustered nanoparticle systems under weakly attractive to highly attractive interactions has advantages over stable systems in that clusters can be consolidated by gravitational sedimentation [22].

There has been much previous work on the physics of particle aggregation resulting in structures that exhibit fractal dimensions [23, 24], but how this process is related to the particle interaction energies is not well understood. A reversible growth model of particle clustering and fractal dimensions as a function of a finite interparticle binding energy, *E*, was reported earlier [25]. Particle rearrangement was allowed due to the probability of unbinding based on a Boltzmann factor, exp (-*nET*) where *n* is the coordination number of a particle that can be removed from a cluster at binding energy *E* and temperature *T* [25]. A dimensionless quantity, τ_R/τ_D, was introduced where τ_R is the inverse unbinding attempt frequency and τ_D is related to the particle diffusivity. Cluster growth was simulated by the Monte Carlo method as a function of the above parameters and the fractal dimension, *D* was calculated as discussed previously [25].

Figure 5 shows that the fractal dimension, *D*, of clusters simulated by the Monte Carlo method, is greatly affected by the interparticle binding energy. At large *E*, *D* is close to the cluster-cluster aggregation model value [26], but greatly increases below a critical binding energy, *3T*. Clusters with high *D*, therefore, are obtained under weakly attractive conditions and Figure 5 indicates that these clusters exhibit the greatest degree of restructuring, as evidenced by the increase in *D* between 5,000 and 10,000 τ_D. Since D is related to the density of nonuniform objects, this indicates that even in flocculated systems, high cluster densities can be achieved when interactions are weakly attractive and significant restructuring is allowed.

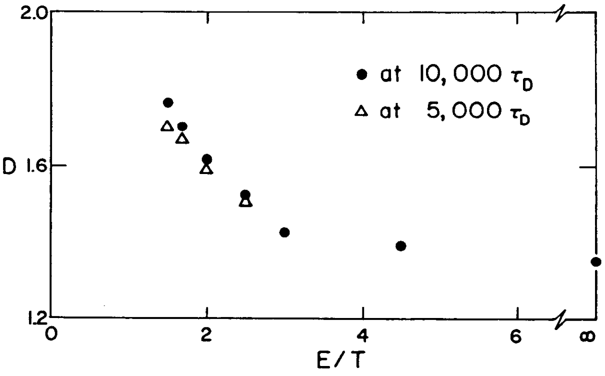

Figure 5. Fractal dimension, *D*, versus *E*/*T* for $\tau_R / \tau_D = 5$ from Ref. [25].

We investigated these trends experimentally in colloidal gold systems [22]. Stable colloidal gold particles were prepared by the reduction of gold chloride with sodium citrate. Particles were aggregated by the adsorption of various types and amounts of surfactants which modified the particle interaction energies [22]. Figure 6 shows clusters dried on carbon grids and observed under TEM as a function of the amount of cationic surfactant added. Since the surfactant is opposite in charge (positive) to the gold

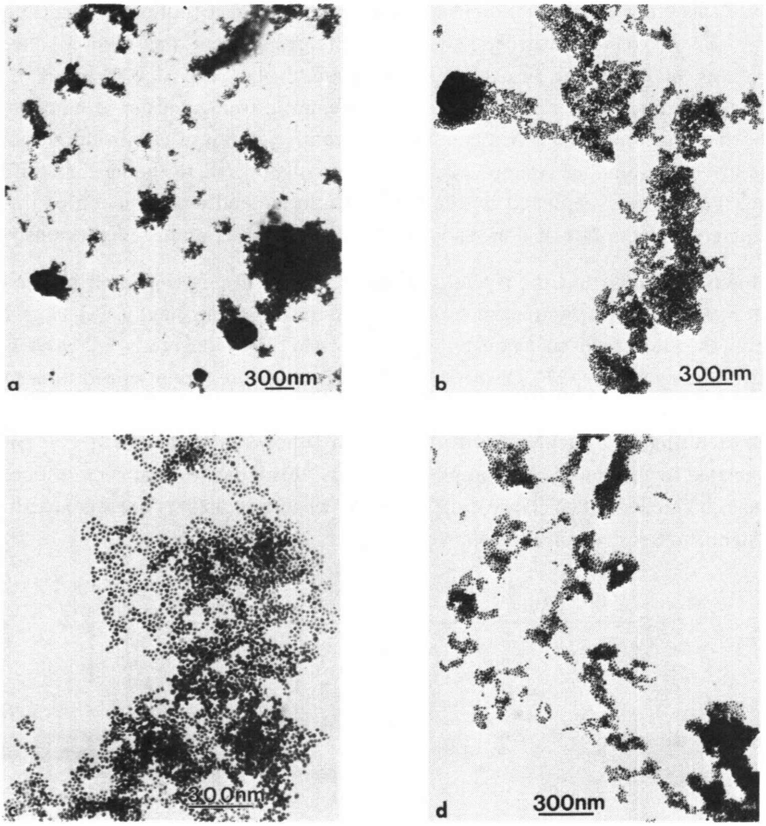

Figure 6. TEM micrographs of aggregate structures as a function of amount of cationic surfactant: (a) 2.33×10^{-5} w/o, (b) 4.67×10^{-5} w/o, (c) 9.33×10^{-5} w/o, and (d) 1.87×10^{-4} w/o.

surface, we expect the surface charge to decrease with increasing amount adsorbed. This would result in increasingly attractive interactions with increasing amount of surfactant.

Figure 6a shows that clusters formed by the adsorption of small amounts of surfactant appear densely packed. Light scattering indicates that these clusters have a high fractal dimension, 2.5, in 3 dimensions. With increasing amount of surfactant, the clusters decrease in density and the fractal dimension drops sharply to 1.9 in Figure 6b and to a minimum of 1.74 in Figure 6c. The experimental data, therefore, corresponds well to the trends predicted by the reversible growth model in Figure 5 where an increase in attraction results in a sharp decrease in fractal dimension. The minimum density in Figure 6c corresponds to a maximum in interparticle binding energy resulting in fast aggregation and fractal dimensions that agree with cluster-cluster models [26] and the reversible growth model [25] for high *E*. This occurs when the adsorption of cationic surfactant causes charge neutralization. Clusters start to increase in density with the increasing surfactant concentrations shown in Figure 6d. This indicates that the particle charge has reversed and attractive interaction energies decrease. These results indicate that by controlling the particle interactions with the amount of adsorbed surfactant, clusters with high densities can be formed when particle unbinding and rearrangement is allowed.

Aggregation can also be induced by the addition of pyridine or NaCl. Figure 7 shows low density clusters formed by the adsorption of pyridine molecules. These types of clusters have very low densities and low fractal dimensions (1.7) as would be expected for attractive particles except that close examination of particle interfaces indicates the formation of interparticle necks or bridges [22]. This results in the formation of irreversible aggregates which cannot restructure. This type of behavior did not occur for particles clustered using cationic surfactants indicating the role of these surfactants in preventing direct particle-particle contact [22]. We have not observed interparticle bridging in aggregated silica particles because it is likely that adsorbed water layers may also prevent direct particle-particle contact.

Our work on the relationships between particle interactions and packing and cluster structures in nanometer particle systems have allowed us to form dense gels and clustered structures by two methods: (1) the use of particle systems that are stable due to short range repulsion and where the hydrodynamic radius is minimized, and (2) the use of particle systems that are flocculated where particle rearrangement is allowed under weakly attractive conditions. In addition to the consolidation of precipitated colloidal particles to form dense gels and structures, we have investigated other novel techniques for the formation of nanometer scale structures involving the simultaneous precipitation and consolidation of inorganic structures within preformed polymer matrices. As discussed in the next section, we pursue this processing concept as a way to easily form and shape gel structures and dry them without cracking.

PRECIPITATION OF SILICA WITHIN HYDROGEL MATRICES

We have developed techniques to form particulate ceramic structures directly within polymer matrix films. Hydrogel matrices are formed as described previously [27], dialyzed in aqueous solutions at various pH values, and placed in solutions of tetraethoxysilane (TEOS). TEOS diffuses into the matrix and reacts internally by hydrolysis of water within the hydrogel. The hydrogels fill with ceramic over time as

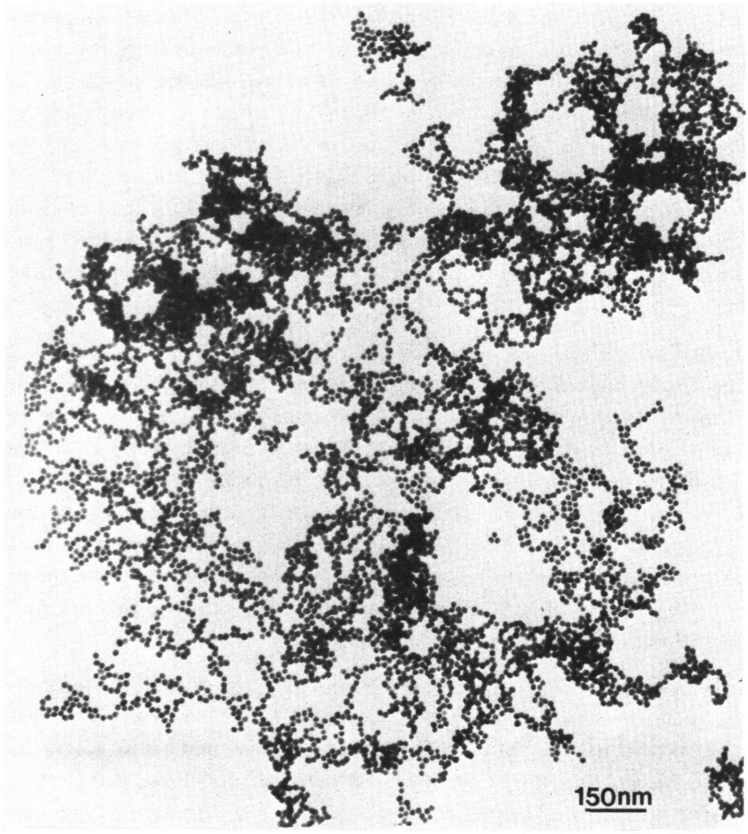

Figure 7. TEM micrograph of aggregate structure formed by addition of pyridine.

evidenced by weight gain data [27] and the rates of weight gain depend on diffusion rates of TEOS within the hydrogel which can be varied by varying the hydrogel pore size.

Microstructures of the silicate-hydrogel composites are shown in Figure 8 for hydrogels treated at pH 7 and pH 3. The microstructures depend on both the silicate reaction chemistry and the hydrogel structure as described in detail previously [27]. pH 7 composites shown in Figure 8a have relatively low silica densities (35 v/o) and have microstructures consisting of uniformly distributed particulate structures with diameters

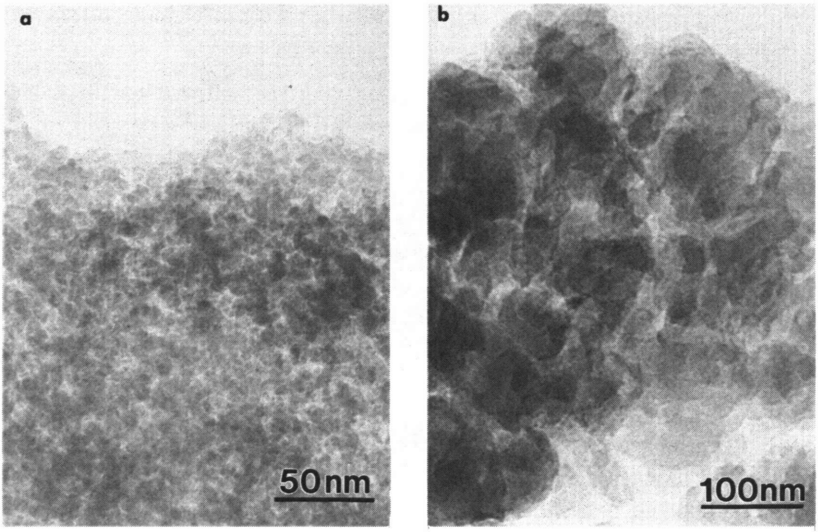

Figure 8. TEM micrographs of gel fragments for hydrogels under (a) neutral pH and (b) acidic acid.

of about 100 Å. These structures correspond to the hydrogel structures at neutral pH where the hydrogels are in swollen states and have uniform polymer networks and small pore sizes [28]. Low overall densities result due to the formation of low density globule type structures similar to the structures seen previously in base catalyzed TEOS systems [28].

Microstructures and silica densities are much different under acid treated pH 3 conditions. TEM micrographs of these composites in Figure 8b show dense silicate regions with a nonuniform distribution of sizes and shapes separated by very low density regions. The silicate structures are much larger (about 400 Å diameter) than the particulate structures under neutral pH conditions. Under high magnification (not shown here), the separated dense regions have fine features less than 10 Å in diameter, similar to structures seen previously under acid catalyzed conditions [29]. Under these conditions, we were able to form dried composite samples with silica volume contents as high as 65 v/o.

The separation and size distribution of the dense regions can be understood by examining the expected hydrogel structure under acidic pH conditions. Placing hydrogels in acidic solutions results in a transition from a swollen state gel with a uniform polymer network and small pores, to a collapsed state gel with a nonuniform, phase separated polymer network with large pores [28]. Structural changes occur because of the changes in hydrogel chemistry. The large, separated silicate regions, therefore, correspond to the large pore sizes between phase separated polymer regions.

It is interesting that the ceramic structure may be controlled by the hydrogel structure on one scale as well as the reaction chemistry on a smaller scale. This indicates that in situ precipitation within polymer matrices is an important technique for microstructural control on a nanometer scale. The use of a polymer matrix also facilitates dissipation of drying stresses as films could be dried easily without cracking. In addition, the polymer could be formed easily to desired shapes and could be burned out to form amorphous films.

CONCLUSIONS

We have presented results on the relationships between particle interactions, microstructures, and packing of nanometer-sized particles and processing directions toward the formation of dense gels and clusters. Studies on silica particles indicate that the hydrodynamic radius due to electrostatic repulsion greatly reduces wet gel packing densities. Dense gels can be achieved when the hydrodynamic radius is minimized and particles are stable due to short-range repulsion. Studies on gold particles indicate that aggregation can be controlled by the use of surfactants, and cluster densities depend on interparticle binding energies. Dense clusters can be formed when particle rearrangement is allowed under weakly attractive interactions. Other techniques involving nanostructure processing include the precipitation of silica within polymer matrices. The polymer has a role in microstructural control and facilitates the drying of gel structures without cracking.

ACKNOWLEDGMENTS

This work was supported in parts by Alzeta Corporation, the Air Force Office of Scientific Research (AFOSR) and Defense Advanced Research Projects Agency (DARPA) under Grant No. AFOSR-87-0114, and Battelle Pacific Northwest Laboratories.

REFERENCES

1. E. A. Barringer and H. K. Bowen, *J. Am. Ceram. Soc.* **65** [12] C199 (1982).
2. I. A. Aksay in ***Advances in Ceramics, Vol. 9,*** edited by J. A. Mangels and G. L. Messing (Am. Ceram. Soc., OH, 1984), p. 94.

3. See articles in ***Science of Ceramic Chemical Processing,*** edited by L. L. Hench and D. R. Ulrich (Wiley, NY, 1986).
4. J. Cesarano III and I. A. Aksay, in press, *J. Am. Ceram. Soc.*, April 1988.
5. E. M. Rabinovitch, D. W. Johnson, J. B. MacChesney, E. M. Vogel, *J. Amer. Ceram. Soc.* **66** [10] 683 (1983).
6. C. J. Brinker, W. D. Drotning, G. W. Scherer, in ***Better Ceramics Through Chemistry, MRS Proc., Vol. 32,,*** edited by C. J. Brinker, D. E. Clark, and D. R. Ulrich (Elsevier Sci. Pub. Co., Inc., NY, 1984) p. 25.
7. D. W. Schaefer and J. E. Martin, *Phys. Rev. Lett.* **52** [26] 2371 (1984).
8. J. Penfold and J. D. F. Ramsay, *J. Chem. Soc. Faraday Trans.* **81,** 117 (1985).
9. J. Th. G. Overbeek in ***Colloid Science, Vol. 1,*** edited by H. R. Kruyt (Elsevier, 1952).
10. J. D. F. Ramsay and B. O. Booth, *J. Chem. Soc. Faraday Trans. I* **79,** 173 (1983).
11. S. Hachisu, A. Kose, Y. Kobayashi, and K. Takano, *J. Colloid. Interface Science* **55** [3] 499 (1976).
12. T. Ohtsuki, A. Kishimoto, S. Mitaku, and K. Okano, *Japanese J. of Appl. Phys.* **20** [3] 509 (1981).
13. S. Hachisu and Y. Kobayashi, *J. Colloid. Interface Sci.* **46** [3] 470 (1974).
14. W. Y. Shih, I. A. Aksay, R. Kikuchi, *J. Chem. Physics* **86** [9] 5127 (1987).
15. B. J. Tarasevich, Master's Thesis, University of Washington (Seattle, 1988).
16. J. Th. Overbeek, *J. Colloid Interface Science* **58** [2] 408 (1977).
17. L. H. Allen and E. Matijevic, *J. Colloid Interface Sci.* **31** [3] 287 (1969).
18. J. N. Israelachvili and G. E. Adams, *J. Chem. Soc. Faraday Trans. I* **74** 975 (1978).
19. N. V. Churaev and B. V. Derjaguin, *J. Colloid Interface Sci.* **103** [2] 542 (1985).
20. C. Aubert and D. S. Cannell, *Phys. Rev. Lett.* **56** [7] 738 (1986).
21. C. J. Brinker in ***Transformation of Organometallics with Common and Exotic Materials: Design and Activation,*** edited by R. M. Laine (Martinus Nijhoff, Dordrecht, 1988), p. 261.
22. J. Liu, M. Sarikaya, and I. A. Aksay, to be submitted for publication.
23. D. W. Schaefer, J. Martin, P. Wiltzius, and D. S. Cannell, *Phys. Rev. Lett.* **52** [26] 2371 (1984).
24. D. A. Weitz and J. S. Huang, in ***Kinetics of Aggregation and Gelation,*** edited by F. Family and D. P. Landau (Elsevier Science Pub., Amsterdam, 1984), p. 19.
25. W. Shih, I. A. Aksay, and R. Kikuchi, *Phys. Rev. A* **36** [10] 5015 (1987).
26. P. Meakin, *Phys. Rev. Lett.* **51,** 1119 (1983).
27. B. J. Tarasevich, I. A. Aksay, and M. Sarikaya, in ***Atomic and Molecular Processing of Electronic and Ceramic Materials, MRS Proc.,*** edited by I. A. Aksay, G. L. McVay, T. G. Stoebe, and J. F. Weger, (Elsevier Sci. Pub. Co., NY, 1988).
28. T. Tanaka, S. Ishiwata, and C. Ishimoto, *Phys. Rev. Lett.* **38** [14] 2916 (1984).
29. C. J. Brinker, K. D. Keefer, D. W. Schaefer, and C. S. Ashley, *J. of Noncrystalline Solids* **48,** 47 (1982).